JOURNAL OF GEOPHYSICAL RESEARCH, VOL. 103, NO. A3, PAGES 4023–4039, MARCH 1, 1998

A statistical study of the ionospheric convection response to changing interplanetary magnetic field conditions using the assimilative mapping of ionospheric electrodynamics technique

A. J. Ridley[1,2] and Gang Lu

High Altitude Observatory, National Center for Atmospheric Research, Boulder, Colorado.

C. R. Clauer and V.O. Papitashvili

Space Physics Research Laboratory, University of Michigan, Ann Arbor.

Abstract. We examine 65 ionospheric convection changes associated with changes in the Y and Z components of the interplanetary magnetic field (IMF). We measure the IMF reorientations (for all but six of the events) at the Wind satellite. For 22 of the events the IMF reorientation is clearly observed by both Wind and IMP 8. Various methods are used to estimate the propagation time of the IMF between the two satellites. We find that using the magnetic field before the IMF orientation change gives the smallest error in the expected propagation time. The IMF is then propagated to the magnetopause. The communication time between when the IMF encounters the magnetopause and the start of the convection change is estimated to be 8.4 ($\pm$8.2) min. The resulting change in the ionospheric potential is examined by subtracting a base potential pattern from the changing potential patterns. From these residual patterns, a number of conclusions are made: (1) the location of the change in convection is stationary, implying that the change in convection is broadcast from the cusp region to the rest of the ionosphere in a matter of seconds and that the elctric field mapped down the cusp controls the entire dayside ionospheric convection pattern; (2) the shape of the change in the ionospheric convection is dependent on the IMF component that changes, which is indicative of the change in the merging rate on the dayside magnetopause; (3) 62% of the events change linearly form one state to another, while 11% of the events change asymptotically; (4) the change in the ionospheric potential is linearly related to the magnitude of the IMF orientation, with B_z changes having a larger proportionality constant than B_y changes; (5) the ionospheric convection takes, on average, 13 min to completely reconfigure; and (6) some of the ionospheric convection changes occur on a timescale shorter than that of the corresponding IMF reorientation, possibly as a result of thresholding in the dayside merging region.

1. Introduction

There are numerous models of steady, high-latitude ionospheric convection [*Heelis*, 1984; *Foster*, 1983; *Friis-Christensen et al.*, 1985; *Heppner, and Maynard*, 1987; *Holt et al.*, 1987; *Richmond, and Kamide*, 1988; *Senior et al.*, 1990; *Papitashvili et al.*, 1994; *Weimer*, 1995; *Ruohoniemi, and Greenwald*, 1996]. Most of these models are parameterized according to the direction and magnitude of the interplanetary magnetic field (IMF) in the Y-Z plane. Such parameterization assumes that the convection is controlled almost exclusively by magnetic field line merging (as first proposed by *Dungey* [1961]). These models agree on the basic structure of the ionospheric convection, for example, the antisunward flow over the magnetic pole when the IMF B_z is southward.

Studying the steady state ionospheric convection may give insight into the merging process, such as where merging takes place [*Crooker*, 1979; *Burch et al.*, 1985; *Reiff, and Burch*, 1985], the role of lobe cell merging [*Crooker, and Rich*, 1993, and references therein], and how B_z northward merging differs from B_z southward merging [*Crooker*, 1992; *Cumnock et al.*, 1992]. Furthermore, information on the ratio of merging potential to viscous interaction potential can be derived from steady state ionospheric convection patterns [*Feldstein, and Levitin*, 1986; *Lu, et al.*, 1994].

A number of studies have been undertaken to describe how the ionospheric convection responds to chang-

[1] Also at Space Physics Research Laboratory, University of Michigan, Ann Arbor.

[2] Now at Southwest Research Institute, San Antonio, Texas.

Paper number 97JA03328.
0148-0227/98/97JA-03328$09.00

ing IMF orientations [*Knipp et al.*, 1991; *Clauer, and Friis-Christensen*, 1988; *Etemadi et al.*, 1988; *Todd et al.*, 1988; *Greenwald et al.*, 1990; *Lockwood et al.*, 1990; *Saunders et al.*, 1992; *Lester et al.*, 1993; *Hairston, and Heelis*, 1995; *Clauer et al.*, 1995; *Stauning et al.*, 1995; *Ridley, and Clauer*, 1996; *Ridley et al.*, 1997]. Most of these studies show that the ionosphere starts to respond 3-10 min after the change in IMF first encounters the magnetopause. Some of them show that the magnetosphere-ionosphere communication time is minimum at the ionospheric projection of the cusp and increases symmetrically toward dawn and dusk [*Etemadi et al.*, 1988; *Todd et al.*, 1988; *Saunders et al.*, 1992]. This increase of the communication time away from the cusp has been interpreted as a possible propagation, or spreading, of the change in convection. The studies further show that the ionosphere takes 10-25 min to fully reconfigure to the change in IMF orientation, although some studies have shown that the convection on the nightside may not develop for up to an hour after the ionosphere starts to reconfigure. Almost all of these results are based on localized observations of the ionospheric convection using radars, magnetometers, and satellites.

Ridley et al. [1997] show six cases of the response of the global electric potential pattern to the IMF orientation changes, using the assimilative mapping of ionospheric electrodynamics (AMIE) technique [*Richmond, and Kamide*, 1988]. That study is different from the above mentioned studies, since global images of the convection are derived, allowing us to globally view the convection changes in the different regions of the ionosphere.

This paper continues the study of ionospheric convection change, started by *Ridley et al.* [1997]. Fifty-nine more events are included in this study. A statistical analysis of how the ionospheric convection responds to changes in the IMF is presented. Included in this study are descriptions of the shape and magnitude of the changes of the ionospheric convection, the evolution of the change, the dependence of the magnitude of the ionospheric convection change on the IMF orientation change, and a study of the various timescales involved and how they relate to each other. These timescales include (1) the propagation time of the IMF from the satellite to the magnetopause, (2) the duration of the IMF change, (3) the magnetopause-ionosphere communication time, (4) the interionospheric communication time, and (5) the ionospheric reconfiguration time.

2. The AMIE Technique

The AMIE technique was used in this study to determine the electric potential in the ionosphere, as was done by *Ridley et al.* [1997]. AMIE has been successfully used in many investigations to examine electrodynamic features in the ionosphere [e.g., *Knipp et al.*, 1991,1993; *Lu, et al.*, 1994, 1995 ; *Taylor et al.*, 1996; *Ridley et al.*, 1998] and readers are referred to these papers and the references therein for a detailed description of the AMIE technique.

A suite of 115 magnetometers to derive the potential patterns for this study. Figure 1 shows the distribution of magnetometers above 50° invariant latitude at 1600 UT. Satellite measurements of electric fields or conductivities have not been included. By including these measurements the convection and/or conductivity may be either enhanced or suppressed in regions surrounding the flight path of the satellite during the 1-min time span in which the potential patterns are calculated. Such alteration would propagate with the satellite along the satellite path, resulting in a distorted convection time series. Radar data have not been included in the study because the temporal resolution of most radar stations is between 2 and 5 min, while this study attempts to resolve 1 min variations. These factors would complicate the studies of the convection changes.

The AMIE technique is limited by the lack of data over large geographic regions (for example, in Figure 1, between 2200 and 0500 MLT). Because of this, statements on small-scale features observed in the AMIE patterns are not discussed in this paper. Furthermore, the majority of the events included in this study occurred when a large number of the magnetometer stations were on the dayside. Some of the events occurred during time periods during which there was a large data gap within a residual potential cell. We have included these events if the residual potential patterns were consistent with other residual patterns derived after similar IMF orientation changes. If a residual potential pattern differed significantly from other residual patterns, while very few data sources were within the cells, the event was discarded.

3. Event Selection

The events in this study were selected by using two methods: (1) Time periods in which there were obvious reorientations of the IMF were sought, such as sign changes in B_z or B_y, and then the ionospheric convection patterns (derived by the AMIE technique) were examined for an ionospheric reconfiguration. (2) Long time series of ionospheric con-

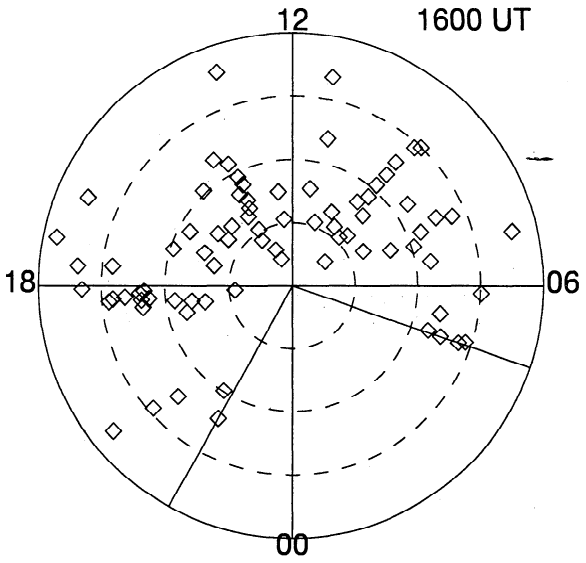

Figure 1. Approximate locations of the magnetometers above 50° invariant latitude used in this study at 1600 UT.

vection patterns (derived by the AMIE technique) were examined for changes in the potential, and then the IMF data were examined. If an obvious IMF orientation change was observed, the event was included; if not, the event was discarded. It should be noted that substorm events were not included in this study. (A large enhancement in AE associated with a large east-west flow in the midnight region is termed a substorm here.) Although there is a significant change in the ionospheric convection during a substorm, the change is usually confined to the nightside. In addition, substorms have not been shown conclusively to be directly associated with IMF orientation changes.

The AMIE technique requires a large quantity of data with good spatial coverage to determine the convection patterns to an accurate degree. This study is therefore limited to two time periods. The first contains six ionospheric convection changes and was the focus of the study presented by *Ridley et al.* [1997]. The other time period, March 15 through April 9, 1995, was selected because there were a large number of sign changes in the IMF B_y and B_z measured by the Wind satellite. A further 59 events are found during this period, for a total of 65. During the March 15 through April 9 time period the Wind satellite was located upstream of Earth by approximately 200 R_E and off the Earth-Sun axis by approximately 30-50 R_E.

Both the IMP 8 and Wind satellites were in the solar wind during 23 of the events. For 22 of these events the changes in IMF were identified at both Wind and IMP 8. These events were used to study different methods of propagating the IMF to the magnetopause. There was only one event in which the Wind and IMP 8 measurements were significantly different. This event was used in the statistical study of the changing convection but was not used to study the IMF propagation. To be consistent, the Wind measurements were used for all of the March and April 1995 events, even though small discrepancies were observed between the two satellites.

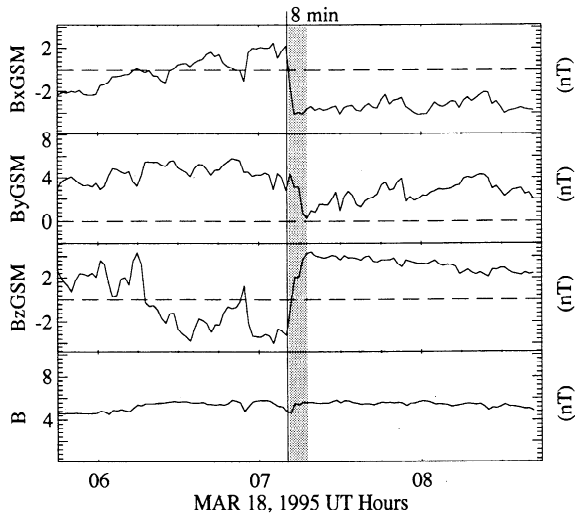

Figure 2. The interplanetary magnetic field (IMF) on March 18, 1995. (top to bottom) B_x, B_y, B_z, and the magnitude of B. The vertical line indicates the start of the IMF orientation change. The grey region shows the time period of the IMF change.

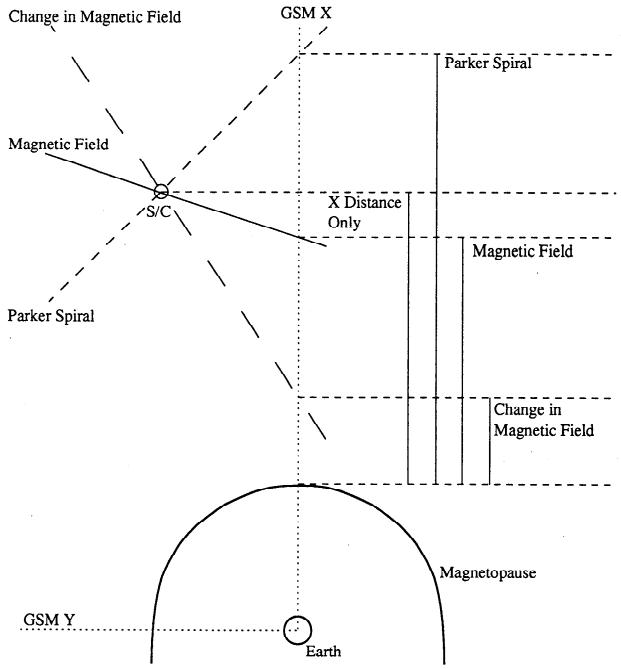

Figure 3. Comparison of different methods of determining the propagation time between a spacecraft (S/C) and the magnetopause. Three lines are drawn through the circle, which represents the S/C. The solid line is the magnetic field (in the X-Y plane) before the reorientation. The short-dashed line is the Parker spiral. The long-dashed line is the change in the magnetic field in the X-Y plane. The distances between the intersections of the three lines at the GSM X line and the magnetopause are indicated by the solid vertical lines. The X distance between the S/C and the magnetopause is also indicated. These distances are divided by the solar wind speed, and four different propagation times are derived.

4. Case Studies

4.1. Positive B_z Turning

Figure 2 shows the IMF on March 18, 1995, from 0545 to 0845 UT, measured by the Wind satellite, which is at (210.7, 24.5, 25.3) R_E in GSM coordinates. At 0711 UT the IMF B_z changes from negative to positive. B_y also changes, but the magnitude of the B_z change is approximately twice as large. In this study we disregard the effect of the X component. The change in B_z occurs over a 7-min period. This reorientation in the IMF causes an ionospheric convection change to occur approximately 68 min later, at 0819 UT.

To determine the time delay between when the IMF first encounters the magnetopause and when the ionosphere starts to reconfigure, the propagation time between the Wind spacecraft and the magnetopause must be estimated. At this time it is not clear how to compute the propagation time in the most accurate and consistent manner. Therefore the propagation time was calculated by using four slightly different techniques. The different methods are demonstrated in Figure 3. The magnetopause standoff distance is calculated by using a simple pressure balance between the solar wind dynamic pressure and the Earth's magnetic field [e.g.,

Sibeck et al., 1991, and references within]. The magnetosheath flow is modeled after the ones described by *Spreiter et al.* [1966]. The slowing of the solar wind through the magnetosheath adds about 4 min to the propagation time for a magnetopause standoff distance of 10 R_E and a solar wind speed of 450 km/s. The different methods of computing the propagation times are as follows (please refer to Figure 3 in addition):

4.1.1. X distance only. The distance between the magnetopause and the satellite along the X axis is used. A propagation time of 61 min is derived for the event shown in Figure 2, implying that the ionosphere starts to react 7 min after the IMF encounters the magnetopause.

4.1.2. Parker spiral. It is assumed that the change in the magnetic field lies in a Parker spiral. The Parker spiral is the statistical average direction which the IMF lies in $-(X, Y, Z) = \pm(-\sqrt{2}, \sqrt{2}, 0)$. The distance between the intersection of the Parker spiral at the X axis and the magnetopause is then used. The propagation time is 68 min with the use of this method, implying a delay between the magnetopause and ionosphere of 0 min.

4.1.3. Magnetic field. The distance between the intersection of the magnetic field (just before the change in orientation) and the X axis and the magnetopause is used to determine the propagation time. In the present case the magnetic field projected in the X-Y plane is used. The field before the change is lying almost in the Y direction exclusively, so the propagation time is 59 min, very similar to the X distance method.

4.1.4. Change in magnetic field. The distance between the intersection of the change in the magnetic field vector at the X axis and the magnetopause is used to calculate the propagation time. This method is similar to a minimum variance technique, where the direction of least change is found and is assumed to be normal to the discontinuity plane. In this case the change in the X-Y plane is almost orthogonal to the Parker spiral, so the propagation time is very short, 49 min. This effect causes the magnetopause-ionosphere communication time to be very long, 19 min.

The first three methods give communication times comparable to those in previous studies [*Clauer, and Friis-Christensen*, 1988; *Etemadi et al.*, 1988]. The change in magnetic field method gives an unusually large result and may not be believable.

Ionospheric potential patterns during this convection change are displayed in Figure 4. Every fourth derived convection pattern is shown. From 0827 until 0839 UT the ionospheric cross polar cap potential decreases. At about 0835 UT a small positive cell begins to grow at 80° invariant latitude and 1300 MLT. This cell appears to be the afternoon cell in a reversed convection pattern.

This change in ionospheric potential is better illustrated when a base (or reference) potential pattern is subtracted from the changing patterns. The subtraction elucidates where and how much the potential is changing. We average together the 0819-0823 UT potential patterns to derive the base pattern. This averaging is done to smooth over localized phenomena which may alter the residual potential patterns. The base potential pattern is displayed in Figure 5a, while the difference patterns (referred to as the residual patterns), are displayed in Figure 5b.

The residual patterns show a reversed two-cell convection pattern developing in the polar cap ionosphere. Both the positive dusk and negative dawn residual cells retain their general shape throughout the change. The maximum residual potential is at 84° invariant latitude and 1400 MLT throughout the entire period, while the minimum residual potential stays at 76° and 0600 MLT. The positive residual cell is larger in magnitude than the negative cell for most of the time period.

When a time series of the residual cross polar cap potential drop is plotted, the change appears to be linear. Figure 6 illustrates this. The residual potential is shown as the solid line. The dashed lines indicate the average residual poten-

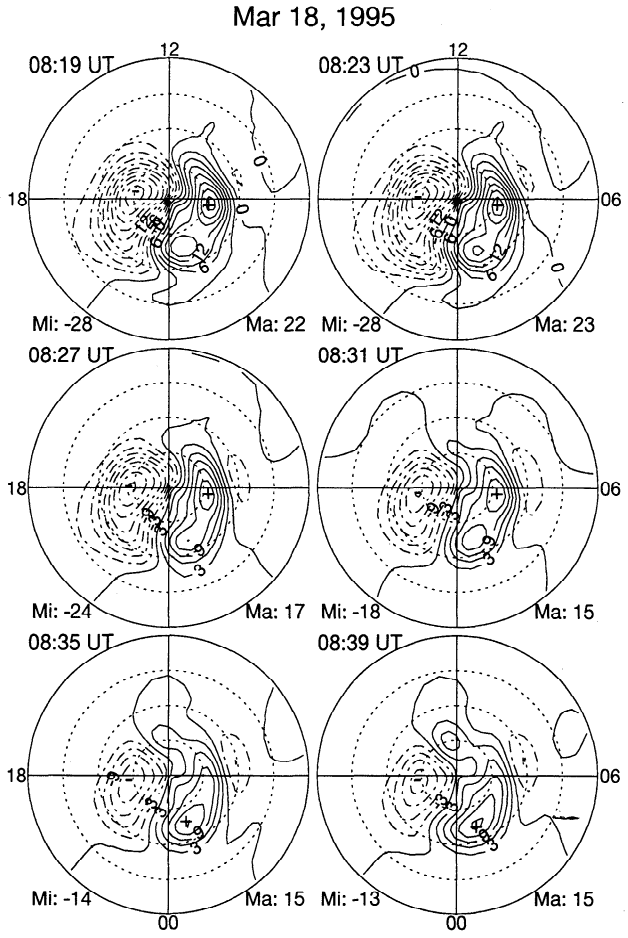

Figure 4. Ionospheric convection during a positive turning in the IMF Z component. The center of each circular plot is the north magnetic pole, while the outer circle is 50° invariant latitude. Magnetic noon is toward the top of each plot, while dawn is to the right. The contours are the electric potential, where the solid lines represent the positive potential and the dashed lines represent the negative potential. The contour interval is 3 kV. The location of the maximum and minimum potential values are represented by a plus and minus sign on the plots, and the value of each is displayed below the plot. "Mi" specifies the minimum potential value, while "Ma" specifies the maximum.

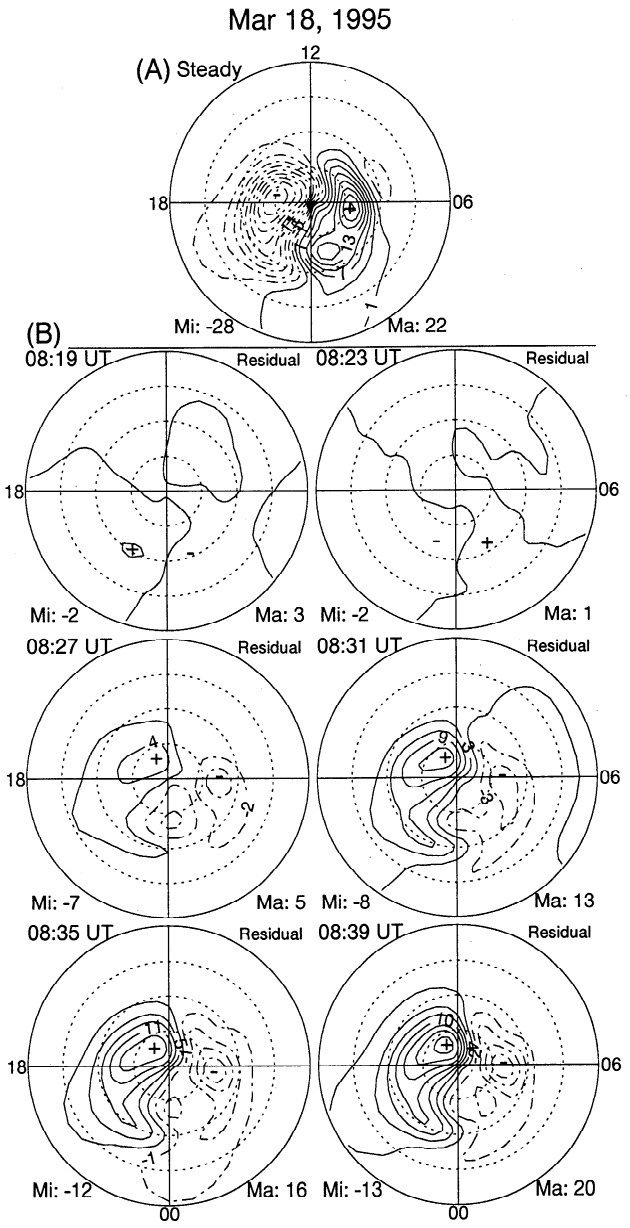

Figure 5. Base potential pattern before the convection change on March 18, 1995, at 0822 UT. This is an average of the 0819-0823 UT potential patterns. It is displayed in the same manner as Figure 4. The residual ionospheric electric potential during a positive turning in the IMF B_z. The contours are the residual electric potential, where the solid (dashed) lines represent positive (negative) changes in the potential. The contour interval is 3 kV. The location of the maximum and minimum residual potential values is represented by a plus and minus sign on the plots, and the value of each is displayed below the plot. "Mi" specifies the minimum potential value, while "Ma" specifies the maximum.

tial values before and after the change, while the dotted line indicates the linear increase in the residual potential. These three lines are fitted to the observed values through an iterative technique in which the summed absolute value difference between the observed values and the lines is minimized. The ionospheric convection starts to change at 0822 UT and becomes steady again at 0839 UT. This behavior implies that

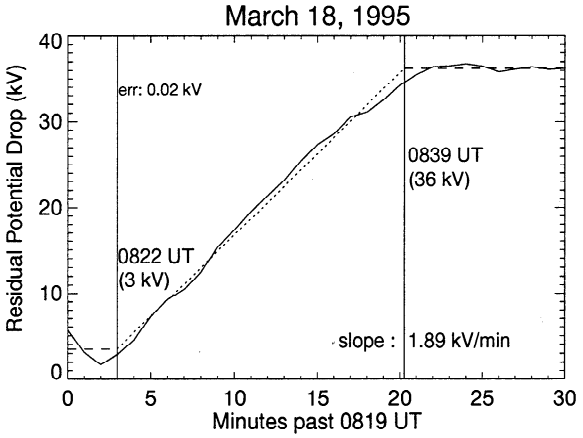

Figure 6. Cross polar cap potential difference of the residual potential patterns in Figure 5b versus time. Some additional times (not shown in Figure 5b) are used to expand the plot. The solid line shows the actual values derived from AMIE. The dashed lines show the steady state values, while the dotted line shows a linear progression between the two steady values (see text for additional information).

the ionosphere takes 17 min to reconfigure and that the increase in the residual potential is 33 kV.

The lack of motion of the residual convection pattern Figure 5 as well as the linear increase in the residual cross polar cap potential drop (Figure 6) is clearly evident. Such features are very similar to those discussed by *Ridley et al.* [1997].

4.2. Negative B_z Turning

The second event, on March 17, 1995, is a southward turning of B_z. The Wind measurements of the IMF are displayed in Figure 7. At 1455 UT, all three components of the IMF change. B_z changes from positive and very close in magnitude to B_y to negative and much larger than the other two components. In this case the B_y change is negligible in comparison with the B_z change. Again B_x is ignored. This re-

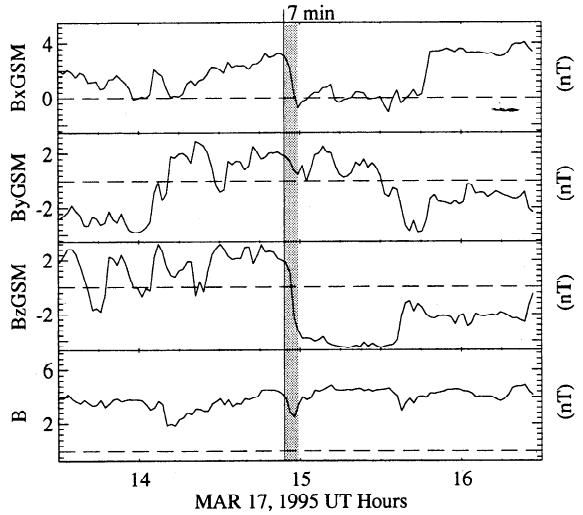

Figure 7. The IMF on March 17, 1995, displayed in the same format as Figure 2.

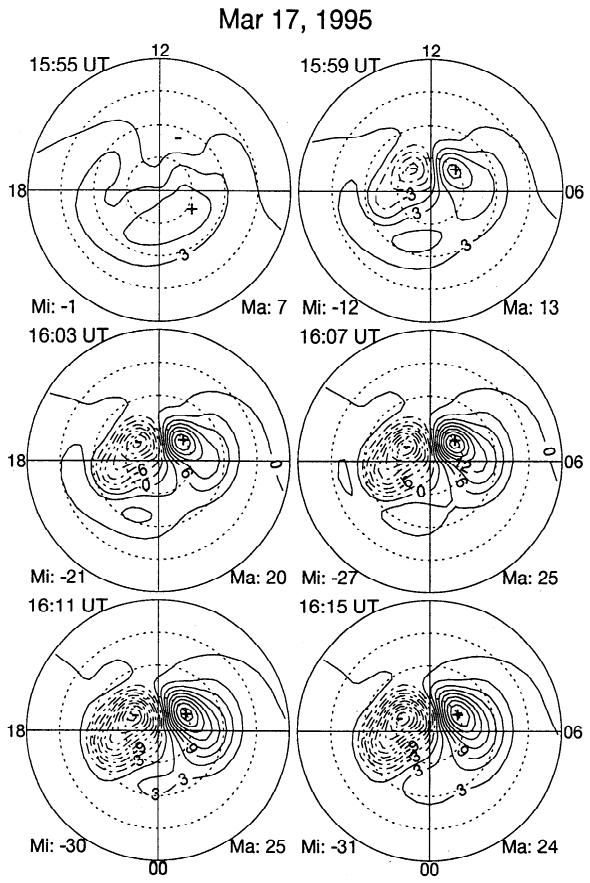

Figure 8. Ionospheric convection during a negative turning of the IMF B_z component displayed in the same format as Figure 4.

orientation of the IMF occurs 61 min prior to the start of the ionospheric reconfiguration, at 1556 UT.

Using the four methods of determining the time delay between when the IMF encounters the magnetopause and when the ionosphere starts to change, we arrive at -9 min for the X distance method, -16 min for the Parker spiral method, and 3 min for the magnetic field and the change in magnetic field methods. (Note that neither the magnetic field nor the change in magnetic field is oriented in the directions indicated by Figure 3 and that a negative time implies that the convection would change before IMF reached the magnetopause.) In this case the magnetic field and change in magnetic field methods give the value closest to those derived in the previous studies [*Clauer, and Friis-Christensen*, 1988; *Hairston, and Heelis*, 1995], while other methods give unrealistic delay times.

The ionospheric convection patterns during the change are displayed in Figure 8. Every fourth derived potential pattern is shown. At 1555 UT the convection is very weak. The following patterns show the standard two-cell convection configuration, with antisunward flow over the polar cap. The cross polar cap potential increases in magnitude from 8 kV before the convection change to 55 kV after the change.

The residual patterns are not displayed, since they are very similar to the potential patterns. The residual potential patterns are observed to retain their general shape throughout the time period of the convection change. The location of the maximum and minimum potential does not change. The negative (dusk) potential cell is slightly larger in magnitude than the dawn cell, which may be caused by the positive B_y. These characteristics are similar to those observed in the previous example and by *Ridley et al.* [1997].

When a time series of the residual cross polar cap potential drop is plotted, as in Figure 9, the change does not appear to be linear, as was shown in the previous example. The solid line represents the AMIE results, while the dotted line represents a fit to the equation

$$\Psi = \Psi_{final}(1.0 - Be^{\frac{t_0 - t}{\tau}}). \quad (1)$$

This equation represents a system that is asymptotically increasing to the final value of Ψ_{final} with an e-folding time constant of τ. B is a normalizing factor, derived so the initial point of the curve matches the steady residual potential before the change. In this case, Ψ_{final} is 58.5 kV and τ is 6.5 min. The ionosphere starts to change at 1556 UT (t_0). These parameters are iteratively derived, so that the summed absolute value difference between the fitted curve and the data points is minimized. We estimate that for this case the change in potential is 50 kV and the time that the ionosphere takes to reconfigure is 13 min. These numbers are derived by determining the final steady residual potential and the time when the residual potential started to oscillate around that value.

It should also be noted that 55 min after this convection change the pattern changes once again, driven by the positive change in B_z (at 1540; see Figure 7). Thirty minutes after that convection change a substorm occurred. We speculate that the magnetosphere-ionosphere system is storing energy after the negative change in B_z. This energy is then released in the form of a substorm. The trigger for the substorm may be the positive change in B_z [*Lyons*, 1996]. The substorm does significantly change the ionospheric convec-

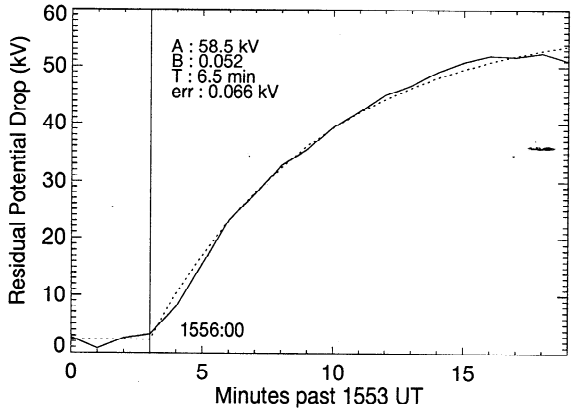

Figure 9. Cross polar cap potential difference of the residual potential patterns from the March 17, 1995, convection change versus time. The solid lines represent the output from the AMIE technique, while the dashed line represents a fitting to an exponential function. The function was fitted iteratively, minimizing the error between the function and the data points.

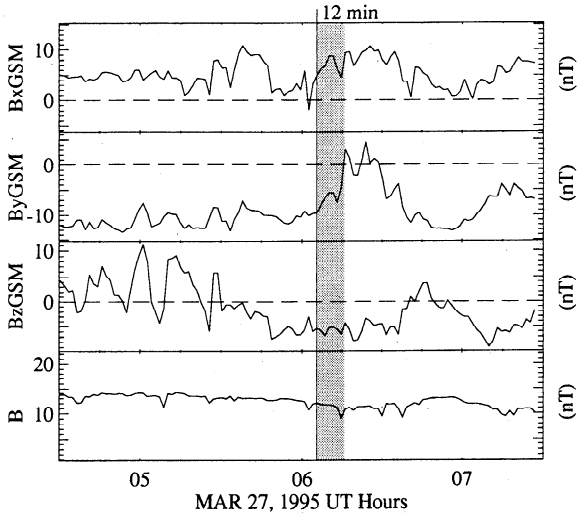

Figure 10. The IMF on March 27, 1995, displayed in the same format as Figure 2.

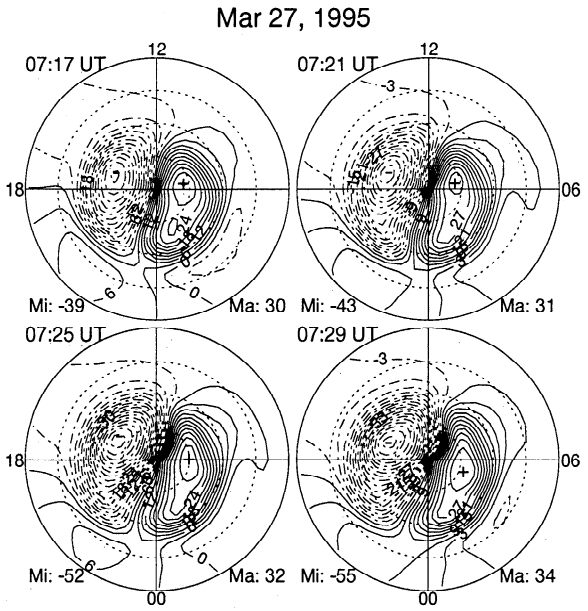

Figure 11. Ionospheric convection during a positive turning of the IMF B_y component on March 27, 1995, displayed in the same format as Figure 4.

tion, but it is not included in the statistical study, since there was no change in the IMF directly associated with the convection change and there is no change in the convection on the dayside.

4.3. B_y Change

The third example, on March 27, 1995, is a change in B_y, as indicated in Figure 10. In this case B_y starts to change at 0605 UT, taking approximately 12 min to change from -10 nT to 1 nT. B_z remains nearly constant throughout this period. The change in B_y causes a change in the ionospheric convection to occur 73 min later, at 0718 UT.

The derived communication times between the magnetopause and ionosphere are 10 min for the X distance method, 0 min for the Parker spiral method, 8 min for the magnetic field method, and 21 min for the change in magnetic field method. As in the first example, the first three methods show communication times consistent with past studies, while the change in magnetic field method shows a possibly unrealistic value.

The potential patterns for this event are displayed in Figure 11. The convection pattern is much larger in both spatial scale and magnitude than that in the previous examples. The change is observed as the negative cell encroaching on the positive cell as well as an increase in the cross polar cap potential, with the negative cell growing in magnitude a little more than the positive cell.

The base potential pattern and the residual patterns are shown in Figure 12. The residual potential patterns show a large, round, negative cell on the duskside, with a weaker elongated positive cell on the dawnside. This is similar to a B_y-positive driven potential pattern [*Papitashvili et al.*, 1994]. The negative residual cell remains the same shape and spatial size during the convection change. The minimum in potential remains in a fixed location. The maximum in potential, on the other hand, occurs alternately at one of three stationary peaks in the residual pattern. We attribute this occurrence to AMIE's inability to resolve the peaks.

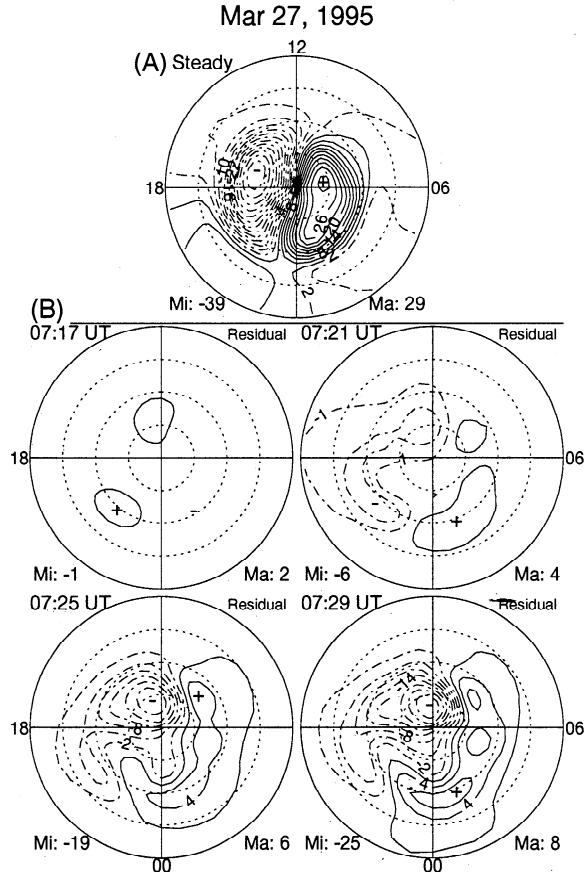

Figure 12. Base potential pattern before the convection change on March 27, 1995, at 0719 UT. This is an average of the 1717-1719 UT potential patterns. It is displayed in the same manner as Figure 4. Residual ionospheric electric potential during a change in the IMF B_y, displayed in the same format as Figure 5b.

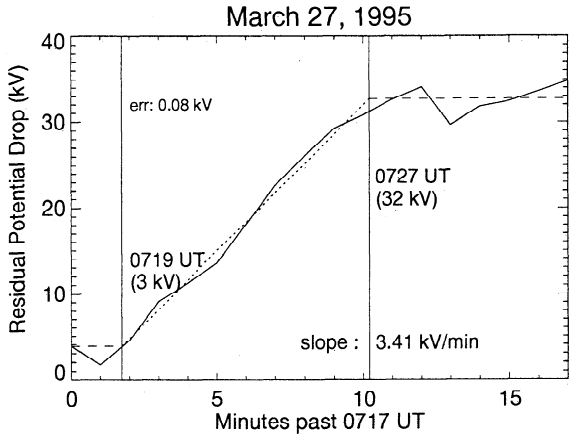

Figure 13. Cross polar cap potential difference of the residual potential patterns in Figure 12b versus time displayed in the same format as Figure 6. Some additional times (not shown in Figure 12b) are used to expand the plot.

When a time series of the residual cross polar cap potential is plotted, the result is again a linear change from one state to another, as shown in Figure 13. This time the potential change is 29 kV over a time period of 8 min. The time of the ionospheric reconfiguration is slightly shorter than the IMF reorientation time, but only by a few minutes. This difference may be attributed to errors in calculating the exact start and stop times of the changes in both the ionospheric convection and IMF orientation.

5. Statistical Study

In general, the events discussed above are typical of the rest of the 65 events examined in this statistical study. In this section we discuss how these events are similar to and different from one another and how the convection changes relate to the IMF conditions.

5.1. IMF Conditions

Figure 14 shows the histogram of the changes in B_z (left) and B_y (middle) for all of the events. Most of the observed events have a change in both the Y and Z components, although the change is often much greater in one component than in the other component. The events are slightly in favor of negative B_z and negative B_y changes. The right plot in Figure 14 gives a histogram of the magnitude of the IMF orientation changes in the Y-Z plane. The magnitude of the IMF change is defined as the magnitude of the difference vector (in the Y-Z plane) between the starting and ending IMF orientations. Events that have changes as low as 2 nT and as high as 25 nT have been examined. The average magnitude change in the Y-Z plane is 6.7 nT. Most of the IMF changes in this study occur in less than 20 min (80%), and all occur in less than 50 min.

5.2. Propagation Between Wind and IMP 8

In 22 of the 65 events examined, both the Wind and IMP 8 satellites are in the solar wind and record similar fluctuations in the IMF. We use these 22 events to help determine which method of propagating the IMF to the magnetopause gives the best result. We do this by propagating the IMF from the Wind satellite to the IMP 8 satellite, using the four methods described in the previous section and comparing these propagation times with the actual observed delay. The difference between the observed and calculated propagation times is given as

$$\Delta t = (t_{IMP8} - t_{Wind}) - t_{prop-time} \qquad (2)$$

where t_{IMP8} and t_{Wind} are the times when IMP 8 and Wind measured the start of the same convection change, respectively, and $t_{prop-time}$ is the propagation time from Wind to IMP 8, determined by the four different methods. A perfect method would have a Δt of zero and a standard deviation (σ) of zero. If the error in the method was somehow systematic, then Δt may turn out to be nonzero, but σ may be small. An unreliable method would have a large σ.

Figure 15 shows the distribution of the Δt values for the four different methods. The mean Δt values and the standard deviations for each method are displayed in each plot. All of the methods overestimate the delay time (a negative time implies that the calculated propagation time is too large). If the methods are evaluated according to the standard deviation of Δt (which is related to the uncertainty in the method), then the magnetic field method appears to be the best, with σ = 8.2 min. The change in magnetic field method is the worst, with σ=13.9 min. The X distance and Parker spiral methods have a σ of 8.6 min and 10.0 min, respectively. All of these σ values are quite large, implying that none of the methods is accurate enough to estimate propagation times to the nearest minute.

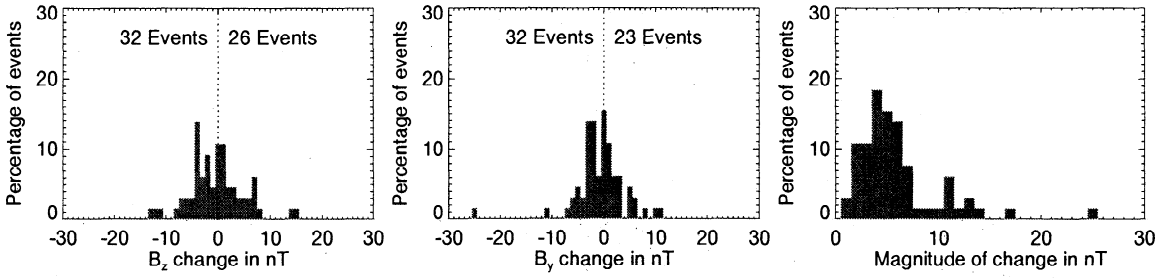

Figure 14. Histogram showing the number of (left) B_z changes, (center) B_y changes, and (right) B changes.

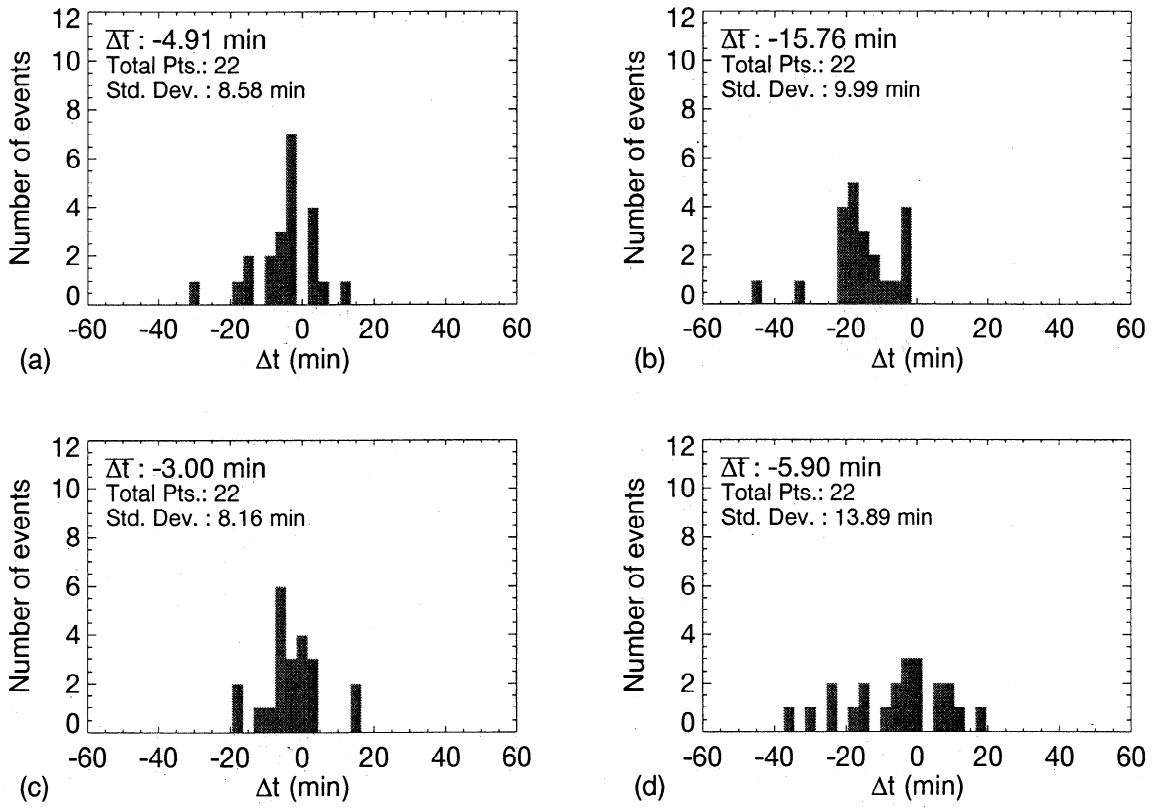

Figure 15. Comparison between actual propagation times measured between Wind and IMP 8 and calculated propagation times using (a) the X distance, (b) the Parker spiral, (c) the magnetic field before the change, and (d) the change in the magnetic field. The average value as well as the standard deviation are given for each method.

In spite of the large uncertainty we next consider the $\overline{\Delta t}$ values, which are the average discrepancy in the propagation method. For the magnetic field method the average discrepancy is -3.0 min, which means that on average the actual propagation of the magnetic field will take 3.0 min less time than the method predicts. The X distance, Parker spiral, and change in magnetic field methods have average discrepancies of -4.9 min, -15.8 min, and -5.9 min, respectively. Understanding the average discrimination in each method is very important in determining time delays between the staellite and the magnetopause.

5.3. Magnetosphere-Ionosphere Communication Time

The communication time between the outer magnetosphere and the ionosphere is an important factor in determining the time scales in which the coupling processes in the magnetosphere-ionosphere system take place. This communication time can be determined by first taking the difference between the start time of the ionospheric reconfiguration and the start time of the IMF reorientation measured at the satellite location, then subtracting the propagation time between the satellite and the magnetopause.

As we discussed in the previous section, the propagation times for the change in IMF from the Wind satellite to the magnetopause can be computed in many different ways. We compare here the statistical results of the magnetopause-ionosphere communication times by using the different methods for propagating the IMF from Wind (or IMP 8, in six cases) to the magnetopause. These results are shown in Figure 16.

The X distance method shows an average magnetosphere-ionosphere communication time of 7.3 min. As we have shown above, from the 22 events in which both Wind and IMP 8 measure the changes, an average underestimation of about -4.9 min is shown to exist. This implies that the IMF propagation takes, on average, 4.9 min less than the expected time. If we take this 4.9-min underestimation into account, the communication time would be 12.2 min, instead of 7.3 min. By incorporating the uncertainty in the method (approximately 8.6 min, according to the σ value in Figure 15) the communication time for the X distance method is 12.2 ($\pm$ 8.6) min. Using this method to compute the magnetospheric-ionospheric communication time for the other three methods, we arrive at 8.4 ($\pm$ 8.2) min for the magnetic field method, 13.5 ($\pm$ 10.0) min for the Parker spiral method, and 13.6 ($\pm$ 13.9) min for the change in magnetic field method.

The average communication times appear slightly longer than those in previous studies, but this fact does not mean this study is inconsistent with the others. For example, *Clauer, and Friis-Christensen* [1988] show a single event that has a communication time of 3 min. This event would fit into the distribution we show, but it is significantly

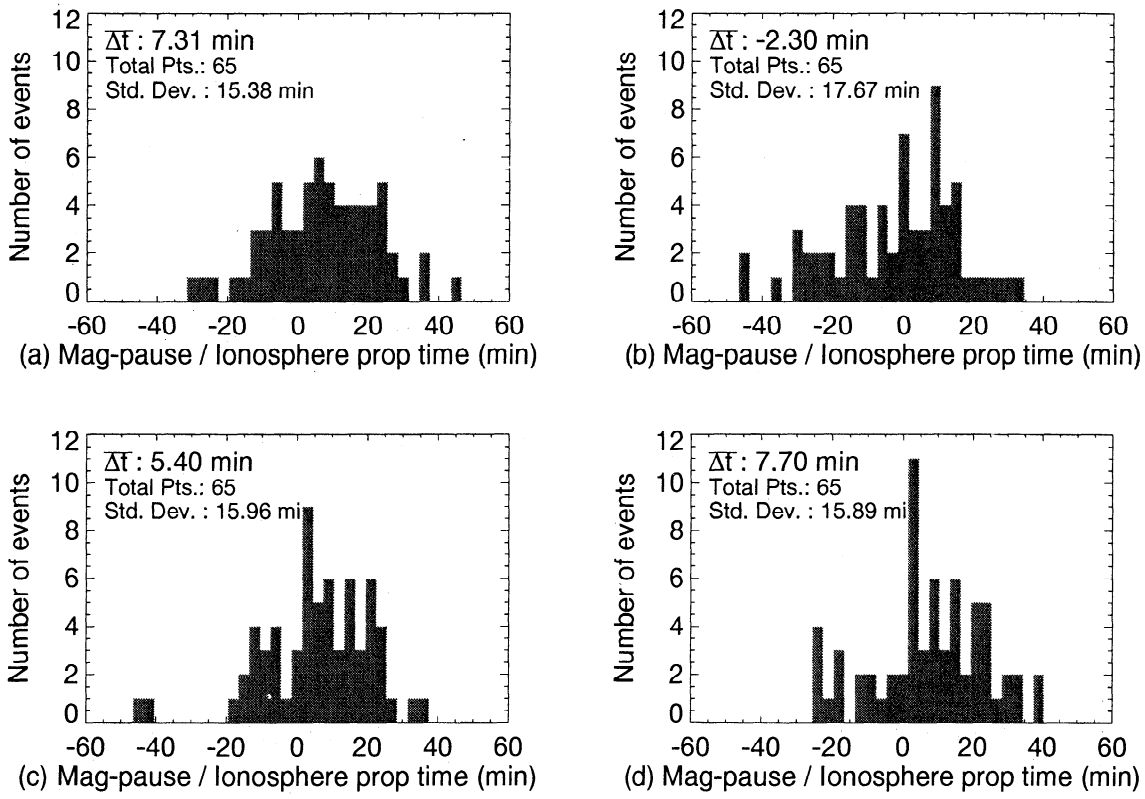

Figure 16. Comparison of the propagation times between the magnetopause and ionosphere using (a) the X distance, (b) the Parker spiral, (c) the magnetic field before the change, and (d) the change in the magnetic field. A negative propagation time would imply that the ionosphere responds to the IMF change before it is estimated to arrive at the magnetopause.

lower than the average communication time. *Etemadi et al.* [1988] and *Todd et al.* [1988] show that the magnetosphere-ionosphere communication time changes with the MLT. If this MLT dependence is ignored and all of the events are grouped together, an average communication time would be approximately 5-10 min. When error bars are included in their cross-correlation studies, an average communication time of 8-14 min is not unreasonable. *Greenwald et al.* [1990] show a number of cases in which the communication time is 8-11 min. *Hairston, and Heelis* [1995] discuss a total of eight convection changes. They propagate the IMF to the magnetosphere, using the Parker spiral method described above, and use the DMSP satellites to determine the minimum start and maximum end time of the convection changes. They show an average communication time of approximately 15 min, consistent with our observations.

Hairston, and Heelis [1995] further discuss a possible difference in timing between northward and southward turnings of the IMF. They show that the ionospheric convection change for the northward turnings of the IMF (positive B_z changes) may take longer to start than those for the southward turnings (negative B_z changes). Although only a small number of events for each type of IMF change are included here (12 for positive B_z changes and 15 for negative B_z changes), the results indicate that positive changes in B_z do not have a longer communication time on average (not shown). There is too much spread in the data along with too few points to make a firm conclusion at this time. This lack of difference in the communication time for southward and northward turnings is consistent with the study of *Ridley, and Clauer* [1996].

5.4. Lack of Motion in the Residual Potential Patterns

In most previous studies on changing convection patterns the change in the convection appears to propagate from the cusp, where it first originates, to the nightside [*Etemadi et al.*, 1988; *Lockwood et al.*, 1990]. In almost all of the events that we examine the residual potential pattern shows very little motion. This lack of motion in the residual potential patterns implies that there is no propagation of the change from the dayside to the nightside. *Greenwald et al.* [1996] present a study of dayside convection vortices, using a pair of Super Dual Auroral Radar Network radars. They find that the vortices evolve (in association with the IMF B_z changes) and disappear (in association with substorm onset) in a fixed postnoon sector. These findings are consistent with the results that we present here.

We conclude that the electric field of the IMF, which is mapped down to the cusp regions, is communicated to the entire polar cap ionosphere in less than 1 min (our temporal resolution). This rapid communication, via a magnetosonic wave traveling at the Alfven velocity, would allow the entire ionosphere to change as a whole and would show no prop-

agation of the changes on the time scale we are observing (e.g., 1 min). The Alfven velocity in the upper ionosphere is approximately 4 orders of magnitude larger than the typical convection velocity of 1 km/s.

This result implies that the solar wind electric field that maps to the cusp controls the entire dayside convection pattern (as described by *Siscoe, and Huang* [1985] and *Lockwood et al.* [1990]). If the localized ionospheric convection were controlled by the solar wind electric field that mapped down the respective field line, the ionopsheric convection would take approximately 1-4 hours to reconfigure (the transit time of a field line across the ionosphere). Because the interionopheric communication time is very fast (less than 1 min), the dayside ionospheric convection must be controlled by the electric field being applied across the cusp.

5.5. Shape of the Residual Potential Patterns

The shape of the residual potential pattern is very much determined by the change in IMF orientation. We discuss three types of IMF orientation changes here: (1) B_y changes with B_z having little to no change and with the magnitude of B_y remaining less than $|B_z|$; (2) B_y changes with B_z having little to no change and the magnitude of B_y becoming either less than or greater than the magnitude of B_z (i.e., the dominant component of the IMF changes), and (3) B_z changes with no significant change in B_y.

If B_y changes while B_z does not and the magnitude of B_y remains less than the magnitude of B_z, the majority of the resulting residual potential patterns are a single cell located on the dayside on the noon-midnight meridian. If the change in B_y is positive (negative), then this potential cell will be negative (positive). The latitude of the center of the cell seems to depend on the sign of B_z. For cases in which B_z is positive the residual potential cell is very close to the pole. When B_z is negative, the center of the residual potential cell is at a lower latitude, near 80°. *Ridley et al.* [1997] illustrate four examples of ionospheric convection changes due to B_y reorientations with a steady B_z positive value. The convection changes in these cases are interpreted as being caused by a change in the east-west direction of the tension on the merged magnetic field lines. Here we verify that the same effect is also true when B_z is negative.

This type of response indicates that the net flux of magnetic fieldlines from the dayside to the nightside is neither increasing or decreasing: it is simply being redirected. This finding suggests that the dayside merging rate may not be controlled by the magnitude of B_y when B_y is not the dominant component of the IMF, since the merging rate in related to the net flux of magnetic field lines from the dayside to the nightside magnetosphere. This result implies that B_y can control the direction of the magnetic field line motion when it has merged but B_z controls that rate of the merging, though only when B_z is the dominant component.

The convection change on March 27, 1995, is an example of the second type of IMF orientation change observed. Before the change the IMF is dominated by a large, negative B_y component. During the change, however, the magnitude of B_y becomes smaller than the magnitude of B_z. The residual potential pattern in the example is two celled. The round negative cell is much larger in magnitude and spatial size than the elongated positive cell. In this type of change the sign of the large round cell is determined by the direction of the change in B_y. There is only a slight difference between these types of convection changes and those in which the dominance of B_z does not change. Instead of a single-cell pattern there are two clear cells in the residual pattern observed, the B_y-dominated round cell and another smaller, yet elongated, cell. This combination of cells is similar to a two-cell B_y dominated convection pattern.

The subtle difference between these residual patterns and the single-cell residual patterns (described above) suggests that when B_y is the dominant component of the IMF it may contribute to determining the merging rate. This is suggested by the change in the amount of magnetic flux being convected from the dayside to the nightside changes during these types of orientation changes (i.e., there is a two-cell residual pattern oriented roughly parallel to the noon-midnight meridian).

For southward IMF B_z changes, but with little to no change in B_y, the residual patterns are two-cell patterns, with both cells being approximately the same magnitude and the positive cell being in the morning sector. This pattern indicates an increase in the amount of magnetic flux being transferred from the dayside magnetopause to the tail. When there is a positive change in B_z, a similar but reversed two-cell residual pattern is observed, with the positive cell being in the afternoon sector. The residual patterns in this case show a decrease in the amount of flux being transported from the dayside to the tail. This decrease in flux transport can cause the net flux transport to become zero. After this, reversed convection starts, and the flux begins transporting from the tail to the dayside magnetosphere.

5.6. Linear and Asymptotically Increasing Convection Changes

In the previous section, two events (on March 18 and March 27) are shown in which the transition from one steady convection pattern to another is linear. The third event (on March 17) shows an asymptotically increasing residual potential drop from one state to another. Overall, 40 events appear to be clearly linear transitions, while eight events have asymptotically increasing residual potentials. In three events it is difficult to determine whether they are linear or asymptotic. The rest of the events (14) are neither linear nor asymptotic, but show a number of different slopes in the transition from one state to the other. We discuss here why the transition from one steady state to another is sometimes linear and sometimes asymptotic.

The eight asymptotically increasing events seem to indicate some type of saturation effect occurring in the magnetosphere-ionosphere system. Previous studies have shown that the polar cap potential can be saturated for very large, negative B_z values [e.g., *Weimer et al.*, 1990; *Reiff, and Luhman*, 1986]. While these studies appear clearly re-

lated to this one, it must be pointed out that the residual potentials are saturating, not the cross polar cap potential. Additionally, the magnitude of B_z is not overly large in the cases presented here.

The shape of the saturation curve is similar to what one would expect in a resistor-capacitor (RC) electric circuit when an electric potential is applied. By using this analogy it is speculated that the magnetosphere-ionosphere system may be storing energy. The asymptotically increasing cases seem to indicate that there may be a saturation in the amount of energy the magnetosphere-ionosphere system can hold, which may be caused by a large discrepancy between the dayside and nightside reconnection rates.

In the linear rise cases the magnetosphere-ionosphere system may be well below the energy storage capacity, thereby showing no signs of saturation. Another possiblity is that the dayside and nightside merging rates do not differ significantly during the transition from one state to another. This similarity would essentially allow magnetic energy to be passed through the system, with no storage occurring at all. For example, if a voltage is applied across a resistor (with no capacitor), and that voltage is increased, the potential drop across the circuit will increase along with the applied voltage and will show no signs of saturation, and no energy will be stored.

In all of the eight asymptotically increasing events a negative change in B_z is observed in the IMF. Southward B_z turnings have been associated with an increase in the size of the polar cap [*Lockwood et al.*, 1990], indicative of a new dayside reconnection rate larger than the tail rate. The resultant energy gained by the tail is usually assumed to be released as a substorm within an hour, but this is true in only a few cases examined (a substorm is identified as a large increase in AE and a convection enhancement in the midnight MLT region in this study). In addition, a number of events with negative B_z changes show a clear, linear change in potential. It is possible that the asymptotically increasing events reflect energy storage, but the subsequent release is often not in the form of substorms.

Another possible explanation for the asymptotically increasing residual potential is that the changes in the magnetosphere-ionosphere system may be occurring on different time scales. For almost all of the convection changes, two processes are occurring simultaneously, namely, the diminishing of one convection pattern and the growth of another. If one of these processes occurs on a shorter time scale than the other, but both are linear and additive, then the resulting growth rate will be steep at first, when both processes are occurring, but will become less steep as the shorter time scale process concludes. This pattern of behavior would give the impression of an asymptotically increasing solution.

5.7. Relationship Between IMF Change and Residual Potential Change

The relationship between the magnitude of the convection change in the ionosphere and the change in the IMF is examined next. Figure 17 shows the change in the residual potential drop against the magnitude of the change of the IMF in the Y-Z plane for all events. The magnitude of the IMF change is defined as the magnitude of the difference vector (in the Y-Z plane) between the starting and ending IMF orientation. These two quantities appear to be linearly correlated with a correlation coefficient of 0.63. A proportionally factor is determined by using an iterative method, where the error between the fitted and actual values is minimized. In this case the proportionality factor is determined to be 3.38 kV/nT, while the error is 0.38 kV/nT. These values pass a 97.5% confidence level test.

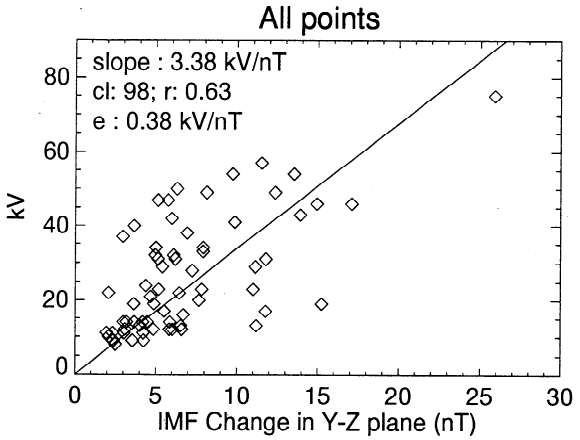

Figure 17. Relationship between the change in residual potential and the magnitude change of the IMF in the Y-Z plane, where "cl" denotes the confidence level, "r" denotes the linear correlation coefficient, and "e" denotes the derived error in the slope.

In the next group of plots, shown in Figure 18, the changes in the IMF orientation are split into changes in B_z (top) and B_y (bottom). A change in B_z is defined as $|\delta B_z| > 2|\delta B_y|$. A change in B_y is then defined as $|\delta B_y| > 2|\delta B_z|$.

The top left plot is a grouping of all the B_z changes, while the top right plot splits these further into negative change in B_z and positive changes in B_z. When all B_z changes are considered, the proportionality between the magnitude of the IMF change and the potential change in the ionosphere increases to 3.98 kV/nT, with an error of 0.69 kV/nT. When only negative changes in B_z are considered, the proportionality factor increases to 4.21 kV/nT (±1.20 kV/nT). Positive changes in B_z have a lower proportionality factor, 3.74 kV/nT (±0.83 kV/nT). The difference between positive and negative changes in B_z shown here is statistically insignificant, since the errors for each are rather large.

The bottom plots are for B_y changes. When all B_y changes are considered, the proportionality factor is 2.61 kV/nT (±0.44 kV/nT). This is lower than that found when all changes in IMF are considered. Since there are so few B_y change cases, it is not as meaningful to split them into negative and positive changes as it is in the cases with B_z changes. We therefore do not consider the separation, but include the plot for reference.

It appears that B_y changes have a smaller influence on the ionospheric convection than do B_z changes, possibly as a result of the different way in which the IMF Y and Z com-

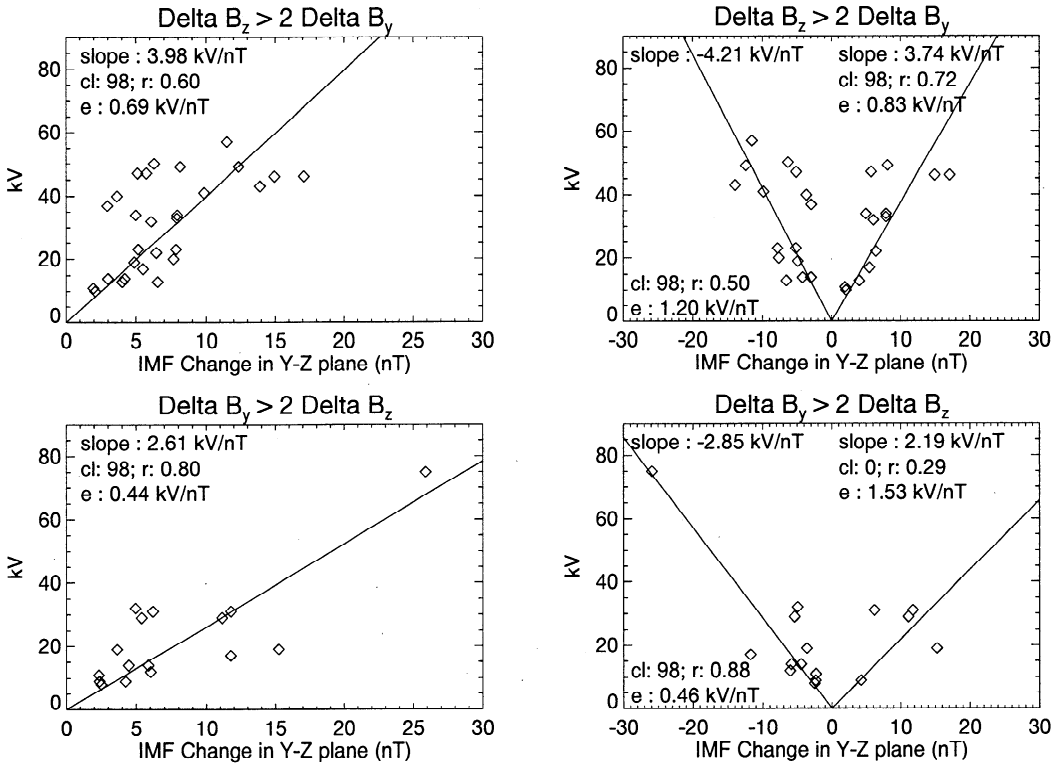

Figure 18. Relationship between the residual potential drop and the magnitude change of the IMF in the Y-Z plane. The top two plots correspond to B_z changes, with the left plot for all B_z changes and the right plot for separated negative and positive changes in B_z. The bottom two plots are for B_y changes. They are in the same format as the B_z changes.

ponents control the merging process between the IMF and the magnetospheric field lines. B_z has typically been associated with controlling the merging rate. However, if the residual potential patterns are examined, it appears here that B_y also plays a role in merging and in the strength of the polar potential (as we discussed in the previous section).

5.8. Ionospheric Reconfiguration Time

Figure 19 shows a distribution of the ionospheric reconfiguration times. The average global ionospheric convection reconfiguration takes approximately 12.6 min. This time is consistent with previous studies [*Clauer, and Friis-Christensen*, 1988; *Hairston, and Heelis*, 1995]. The average ionospheric reconfiguration time is very close to the average IMF reorientation time (13 min).

Figure 20 shows the ionospheric reconfiguration times against the IMF reorientation times for all of the events. The solid line shows where the values would be equal. In gen-

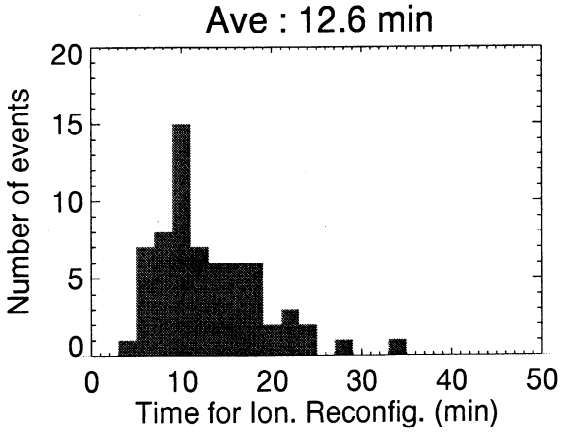

Figure 19. Amount of time the ionosphere took to reconfigure for all IMF orientation changes.

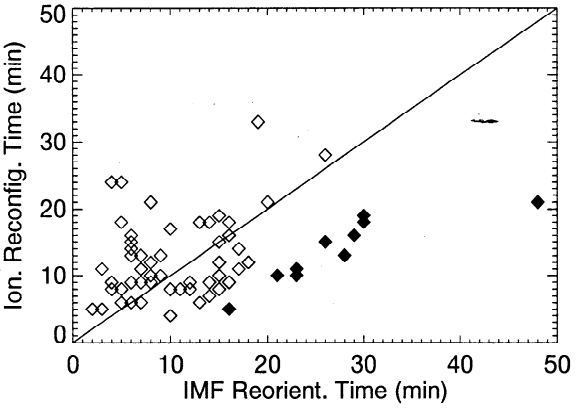

Figure 20. Amount of time the ionosphere took to reconfigure versus amount of time the IMF took to reorient. The solid line represents an equal amount of time. The black solid diamonds are events in which the ionosphere took significantly less time (over 10 min less) to reconfigure than the IMF took to reorient.

eral, the points fall within a few minutes of the solid line, implying that the ionosphere takes about as long to reconfigure as the IMF takes to reorient. For those points above the line the ionosphere takes longer to reconfigure than the IMF takes to reorient. These are usually the cases when the change in IMF are relatively abrupt (less than 10 min). It is expected that for rapid IMF orientation changes the response of the magnetosphere-ionosphere system will be gradual because of its inertia. The points below the line, on the other hand, are those in which the ionosphere takes less time to reconfigure than the IMF takes to reorient.

Ridley et al. [1997] explain this behavior as being due to a merging threshold. In this hypothesis, as the IMF rotates, the merging region may not start to react until the angle between the Z direction and the projection of the IMF in the Y-Z plane passes through some critical value $\delta\theta$. In this statistical study we reach a similar, but slightly modified, conclusion.

It appears that most, but not all, of the long-duration IMF reorientations do not occur at a steady rate. For example, Figure 10 shows an IMF change that occurs over a longer period (12 min) than the corresponding ionospheric reconfiguration (8 min). The start time of the IMF reorientation is marked where B_y starts to increase from the "steady" value. This change is gradual at first, but at 0612 UT, B_y changes very quickly. This start of the rapid rise in B_y may have been the trigger for the merging region to start changing. One of the cases discussed by *Ridley et al.* [1997] shows a B_z change occurs over a 45-min period. The corresponding ionospheric reconfiguration time is approximately 20 min. This B_z change also shows high frequency variations on top of the gradual change. It is possible that one of the sudden increases in B_z triggers the change in merging region.

If this hypothesis were true, then the delayed merging reaction would appear as a longer than normal communication time between the magnetopause and the ionosphere. We therefore recompute the communication times for those events in which the IMF takes longer to reorient than the ionosphere takes to reconfigure by subtracting one half the IMF change time. The new histogram of communication times is shown in Figure 21. In comparison with Figure 16 (the bottom left plot) the average time is decreased by about 2 min. This results in a communication time of 6.2 min (after the Wind to IMP 8 discrepancy of -3 min is subtracted). This communication time is much closer to that in previous studies [*Hairston, and Heelis*, 1995; *Etemadi et al.*, 1988; *Todd et al.*, 1988; *Clauer, and Friis-Christensen*, 1988].

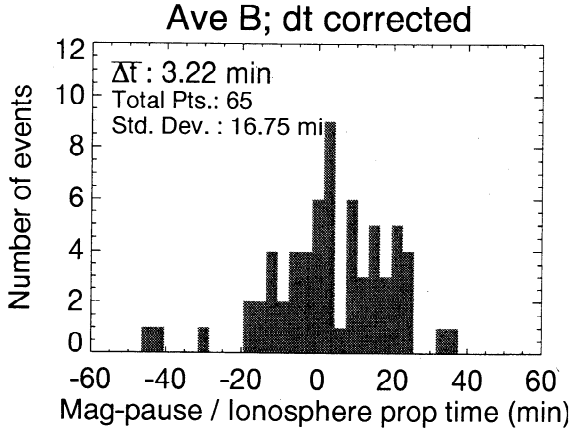

Figure 21. Distribution of the magnetosphere-ionosphere communication times after subtracting half the amount of time the IMF took to reorient for all of the events in which the IMF took longer than the ionosphere to change.

6. Summary and Conclusions

We have examined how the ionospheric potential responds to changes in the IMF B_z and B_y for 65 events. We define a change in one component of the IMF if it is at least twice as large as that of the other component. When this criteria is used, there are a total of 16 events corresponding to B_y changes and 28 corresponding to B_z changes. The changes in B_y and B_z are approximately equal in magnitude for the rest of the events.

We measure the IMF reorientations (for all but six of the events) at the Wind satellite, which is upstream of the magnetosphere at approximately 200 R_E and off the Earth-Sun line toward dusk by approximately 40 R_E. For 22 of the events the IMF reorientation is clearly observed by both Wind and IMP 8. Various methods are used to estimate the propagation time of the IMF between the two satellites. The different propagation methods are tested against the observed propagation times. We have found that using the magnetic field before the IMF orientation change gives the smallest average difference between the observed and calculated arrival time (-3.0 min). This method also gives the smallest standard deviation (8.2 min). Using the Parker spiral before the change seems to give the largest difference (-15.8 min), with a standard deviation of 10.0 min. This may be caused by a large number of events in which the IMF is oriented orthogonal to the Parker spiral. When the X distance method is used, the difference between the observed and calculated propagation times is approximately -4.9 min with a standard deviation of 8.6 min. Using the change in the magnetic field method, we find that the standard deviation is 13.9 min, while the average difference between the observed and calculated propagation times is -5.9 min.

All of these methods have large standard deviations, an implication that none of the methods provides consistent reliable results, although using the magnetic field before the IMF change results in the least amount of uncertainty in the propagation time estimate (i.e., lowest standard deviation). The large uncertainty in the different methods makes it very difficult to estimate an accurate magnetosphere-ionosphere communication time. We conclude that more studies on propagating the IMF from one source to another need to be done before an accurate method can be determined.

We then examine the magnetopause-ionosphere communication time, i.e., the amount of time to communicate the change in the IMF orientation from the magnetopause to the ionosphere. We determine this time by subtracting the time when the IMF encounters the magnetopause, determined by propagating the IMF from the satellite, from the start time of the ionospheric reconfiguration. We find that the four commonly used methods tend to overestimate the propagation time by 3-16 min (when Wind is off the Sun-Earth line by

20-40 R_E). By taking this overestimation into account we estimate that the communication time is between 8.4 (± 8.2) min (for the magnetic field propagation method) and 13.6 (± 13.9) min (for the change in the magnetic field method). This is larger than that in previous results by *Clauer, and Friis-Christensen* [1988] but is not inconsistent with the results of *Etemadi et al.* [1988], *Todd et al.* [1988], and *Hairston, and Heelis* [1995]. We show that there is no clear difference in the communication times for northward and southward turnings of the IMF, as was reported by *Hairston, and Heelis* [1995].

The change in the ionospheric potential is examined by subtracting a base potential pattern from the changing potential patterns. The residual potential patterns clearly show how the convection pattern is changing. We show that the shape of the residual potential pattern is determined by the change in the IMF. Three types of residual potential patterns are observed:

1. A single positive or negative cell centered on the noon meridian is formed by a change in B_y (with no significant change in B_z), but with $|B_z|$ larger than $|B_y|$ before and after the change. The sign of the potential cell is determined by the direction of the change in B_y. A positive (negative) residual potential cell results when the B_y change is negative (positive). The latitude of the cell center appears to depend on the sign of B_z.

2. A very large round cell and an elongated cell result when B_y changes (with no significant change in B_z) and the IMF changes from being dominated by B_z to B_y or by B_y to B_z. The sign of the large round potential cell is determined by the direction of the change in B_y, as in the previous case.

3. Two potential cells with the positive cell in the morning sector and the negative cell in the afternoon sector, approximately equal in size and magnitude, form when there is a negative change in B_z. The two cells are reversed for positive changes in B_z. Differences in the magnitudes of the cells have been attributed to B_y being nonzero.

In all of the residual potential patterns, little motion is observed during the convection change. This finding is different from that of past studies, which show convection changes spreading out from the cusp [e.g., *Saunders et al.*, 1992], but is consistent with the intensification of localized field-aligned currents, as described by *Banks et al.* [1984] and *Clauer, and Banks* [1986]. The lack of motion is attributed to a very rapid ionospheric communication time (possibly via magnetosonic waves traveling at the Alfven speed), so when the IMF electric field is mapped to the ionospheric projection of the cusp, the entire ionosphere reacts to the electric field within a few seconds. The Alfven wave speed in the upper ionosphere is approximately 4 orders of magnitude larger than the convection velocity. This result is a verification of the earlier work by *Siscoe, and Huang* [1985] and *Lockwood et al.* [1990], who stated that the electric field mapped along the cusp specifies the entire dayside ionospheric convection.

When a time series of the residual cross polar cap potential is plotted, a linear change from one state to another is observed 62% of the time. In other events (11% of them) an asymptotically increasing change is observed. Two possible explanations for the asymptotically increasing solution are offered: (1) the magnetosphere-ionosphere system is storing energy, and saturating, in a way analogous to a resistor-capacitor electric circuit storing energy, and (2) two linear changes are occurring simultaneously on different time scales, so that when they are added together, an asymptotically increasing solution results. All of the asymptotically increasing changes correspond to negative changes in B_z, though a number of the linear changes also result from negative changes in B_z. Some convection changes (22% of them) were irregular and could not be classified as either linear or asymptotic for reasons yet to be explored.

The change in the residual potential is compared with the magnitude of the IMF orientation change in the Y-Z plane. When all of the events are combined, the magnitude of the residual potential is shown to be linearly dependent on the IMF change with a proportionality factor of 3.38 (± 0.38) kV/nT. When changes in the individual components are examined, the proportionality factor changes to 3.98 (± 0.69) kV/nT for changes in B_z and 2.61 (± 0.30) kV/nT for changes in B_y. The difference between B_y and B_z change cases may be due to how the components control the merging process at the dayside magnetopause, with B_z controlling the reconnection rate and B_y controlling the direction of the flow in the merging region. By examining the residual potential patterns, however, we find that B_y may affect the merging rate when the dominant component of the IMF switched from B_z to B_y.

By examining the residual cross polar cap potential drop against time it is easy to determine how long the ionosphere takes to reconfigure on a global scale. We show that the ionosphere takes, on average, about 12-13 min to fully reconfigure (excluding substorms). This finding is consistent with the ones of previous studies [*Clauer, and Friis-Christensen*, 1988; *Hairston, and Heelis*, 1995; *Ridley, and Clauer*, 1996]. We further show that some of the ionospheric convection changes occur on a shorter time scale than that of the corresponding IMF reorientation. A number of ionospheric convection changes (approximately 15%) occur on a time scale that we consider much shorter than that of the IMF reorientation. We suggest that the short time scale can be determined by thresholding of the IMF change during the merging process such that the IMF must rotate (in the Y-Z plane) through a certain angle in order for the merging region to start to change. We further suggest that this thresholding may also result from the rate of change of the IMF components.

Acknowledgments. We would like to thank Art Richmond for his insightful thoughts. The data used for this study was provided by a number of different sources. The Greenland magnetometer data were supplied by Eigil Friis-Christensen at the Danish Meteorological Institute. The CANOPUS instrument array was constructed and is maintained and operated by the Canadian Space Agency. The International Monitor for Auroral Geomagnetic Effects (IMAGE) is a joint European project for establishing and maintaining a network of digital magnetometers from southern Finland to the northern part of Svalbaard (H. Lühr, Institute for Geophysics and Meteorology, Germany, and L. Hakkinen, Finnish Meteorological Institute). The SAMNET magnetometer data was supplied by Marc Lester at the Department of Physics and Astronomy, University of Leicester. The Norway magnetometer data was sup-

plied by the Auroral Observatory of Tromso. The 210 Meridian magnetometer data was supplied by K. Yumoto at Kyushu University (principal investigator of the 210MM project), Kyushu, Japan. The Intermagnet magnetometer data is available via CD ROM, and is supplied by the National Geomagnetic Information Center, U.S. Geological Survey (Golden, CO). The NGDC magnetometer data was supplied by Leslie Morris at the World Data Center. DMSP particle, drift meter, and hemispheric power index data was provided by Fred Rich at Phillips Laboratory on Hanscom Air Force Base. The IMP 8 and Wind magnetic field data has been provided by Ron Lepping at NASA Goddard, and the plasma data has been provided by Alan Lazarus at MIT. The Sondrestom upper atmospheric research facility in Kangerlussuaq, Greenland, is managed and operated jointly for the National Science Foundation and Danish Meteorological Institute by SRI International. This work has been supported at the University of Michigan by NSF grants ATM-9412390, ATM-9501380, and OPP-9318766 and at the High Altitude Observatory (HAO) by NSF grant SA93-SFA.1. One of the authors (A.J.R.) was supported by a Newkirk Fellowship at HAO. The Editor thanks H. Koskinen and another referee for their assistance in evaluating this paper.

References

Banks, P.M., T. Araki, C.R. Clauer, J.P. St. Maurice,, and J.C. Foster, The interplanetary magnetic field, cleft currents, and plasma convection in the polar caps, *Planet. Space Sci., 32*, 1551, 1984.

Burch, J.L, P.H. Reiff, J.D. Menietti, R.A. Heelis, W.B. Hanson, S.D.Shawhan, E.G. Shelley, M. Sugiura, D.R. Weimer,, and J.D. Winningham, IMF B_y-dependent plasma flow and Birkeland currents in the dayside magnetoshpere, 1, Dynamics Explorer observations, *J. Geophys. Res., 90*, 1577, 1985.

Clauer, C.R., and P.M. Banks, Relationship of the interplanetary electric field to the high-latitude ionospheric electric field and currents: Observations and model simulation, *J. Geophys. Res., 91*, 6959, 1986.

Clauer, C.R., and E. Friis-Christensen, High-latitude dayside electric field and currents during strong northward interplanetary magnetic field: Observations and model simulation, *J. Geophys. Res., 93*, 2749, 1988.

Clauer, C.R., P. Stauning, T.J. Rosenberg, E. Friis-Christensen, P.M. Miller,, and R.J. Sitar, Observations of a solar-wind-driven modulation of the dayside ionospheric DPY current system, *J. Geophys. Res., 100*, 7697, 1995.

Crooker, N.U., and F.J. Rich, Lobe cell convection as a summer phenomenon, *J. Geophys. Res., 98*, 13,403, 1993.

Crooker, N.U., Dayside merging and cusp geometry, *J. Geophys. Res., 84*, 951, 1979.

Crooker, N.U., Reversed convection, *J. Geophys. Res., 97*, 19,363, 1992.

Cumnock, J.A., R.A. Heelis,, and M.R. Hairston, Response of the ionospheric convection pattern to a rotation of the interplanetary magnetic field on January 14, 1988, *J. Geophys. Res., 97*, 19,449, 1992.

Dungey, J.W., Interplanetary magnetic field and the auroral zones, *Phys. Rev. Lett., 93*, 47, 1961.

Etemadi, A., S.W.H. Cowley, M. Lockwood, B.J.I. Bromage, D.M. Willis,, and H. Lühr, The dependence of high-latitude dayside ionospheric flows on the north-south component of the IMF: A high time resolution correlation analysis using Eiscat "POLAR" and AMPTE UKS and IRM data, *Planet. Space Sci., 36*, 471, 1988.

Feldstein, Y.I., and A.E. Levitin, Solar wind control of electric fields and currents in the ionosphere, *J. Geomagn. Geoelectr., 38*, 1143, 1986.

Foster, J.C., An empirical electric field model derived from Chatanika radar data, *J. Geophys. Res., 90*, 981, 1983.

Friis-Christensen, E., Y. Kamide, A.D. Richmond,, and S. Matsushita, Interplanetary magnetic field control of high-latitude electric fields and currents determined from Greenland magnetometer chain, *J. Geophys. Res., 90*, 1325, 1985.

Greenwald, R.A., K.B. Baker, J.M. Ruohoniemi, J.R. Dudeney, M. Pinnock, N. Mattin, J.M. Leonard,, and R.P. Lepping, Simultaneous conjugate observations of dynamic variations in high-latitude dayside convection due to changes in IMF B_y, *J. Geophys. Res., 95*, 8057, 1990.

Greenwald, R.A., J.M. Ruohoniemi, W.A. Bristow, G.J. Sofko, J.-P. Villain, A. Huuskonen, S. Kokubun,, and L.A. Frank, Mesoscale dayside convection vortices and their relation to substorm phase, *J. Geophys. Res., 101*, 21,697, 1996.

Hairston, M.R., and R.A. Heelis, Response time of the polar ionospheric convection pattern to changes in the north-south direction of the IMF, *Geophys. Res. Lett., 22*, 631, 1995.

Heelis, R.A., The effects of interplanetary orientation on dayside high-latitude convection, *J. Geophys. Res., 89*, 2873, 1984.

Heppner, J.P., and N.C. Maynard, Empirical high-latitude electric field models, *J. Geophys. Res., 92*, 4467, 1987.

Holt, J.M., R.A. Wand, J.V. Evans,, and W.L. Oliver, Empirical models for the plasma convection at high latitudes from Millstone Hill observatory, *J. Geophys. Res., 92*, 203, 1987.

Knipp, D.J., A.D. Richmond, B. Emery, N.U. Crooker, O. de la Beaujardière, D.S. Evans,, and H.W. Kroehl, Ionospheric convection response to changing IMF direction, *Geophys. Res. Lett., 18*, 721, 1991.

Knipp, D.J., et al., Ionospheric convection response to slow, strong variations in a northward interplanetary magnetic field: A case study for January 14, 1988, *J. Geophys. Res., 98*, 19,273, 1993.

Lester, M., O. de la Beaujardière, J.C. Foster, M.P. Freeman, H. Lühr, J.M. Ruohoniemi,, and W. Swider, The response of the large scale ionospheric convection pattern to changes in the IMF and substorms: Results from the SUNDIAL 1987 campaign, *Ann. Geophys., 11*, 556, 1993.

Lockwood, M., S.W.H. Cowley,, and M.P. Freeman, The excitation of plasma convection in the high-latitude ionosphere, *J. Geophys. Res., 95*, 7961, 1990.

Lu, G., et al., Interhemispheric asymmetry of the high-latitude ionospheric convection pattern, *J. Geophys. Res., 99*, 6491, 1994.

Lu, G., et al., Characteristics of ionospheric convection and field-aligned current in the dayside cusp region, *J. Geophys. Res., 100*, 11,845, 1995.

Lyons, L.R., Substorms: Fundemental observational features, distinction from other disturbances, and external triggering, *J. Geophys. Res., 101*, 13,011, 1996.

Papitashvili, V.O., B.A. Belov, D.S. Faermark, Y.I. Feldstein, S.A. Golyshev, L.I. Gromova,, and A.E. Levitin, Electric potential patterns in the northern and southern polar regions parameterized by the interplanetary magnatic field, *J. Geophys. Res., 99*, 13,251, 1994.

Reiff, P.H., and J.L. Burch, IMF B_y-dependent plasma flow and Birkeland currents in the dayside magnetopause, 2, A global model for nothward and southward IMF, *J. Geophys. Res., 90*, 1595, 1985.

Reiff, R.H., and J.G. Luhman, *Solar wind control of the polar-cap voltage*, in Solar Wind-Magnetosphere Coupling, *edited by Y. Kamide and J.A. Slavin*, Terra Sci., Tokyo, 1986.

Richmond, A.D., and Y. Kamide, Mapping electrodynamic features of the high-latitude ionosphere from localized observations: Technique, *J. Geophys. Res., 93*, 5741, 1988.

Ridley, A.J., and C.R. Clauer, Characterization of the dynamic variations of the dayside high-latitude ionospheric convection reversal boundary and relationship to interplanetary magnetic field orientation, *J. Geophys. Res.*, *101*, 10,919, 1996.

Ridley, A.J., C.R. Clauer, G. Lu,, and V.O. Papitashvili, Ionospheric convection during nonsteady interplanetary magnetic field conditions, *J. Geophys. Res.*, *102*, 14,563, 1997.

Ridley, A.J., T. Moretto, P. Ernstrom,, and C.R. Clauer, Global analysis of three traveling vortex events during the november 1993 storm using the assimilative mapping of ionospheric electrodynamics technique, *J. Geophys. Res., In Press*, 1998.

Ruohoniemi, J.M., and R.A. Greenwald, Statistical patterns of the high-latitude convection obtained from Goose Bay HF radar observations, *J. Geophys. Res.*, *101*, 21,743, 1996.

Saunders, M.A., M.P. Freeman, D.J. Southwood, S.W.H. Cowley, M. Lockwood, J.C. Samson, C.J. Farrugia,, and T.J. Hughes, Dayside ionospheric convection changes in response to long-period interplanetary magnetic field oscillations: Determination of the ionospheric phase velocity, *J. Geophys. Res.*, *97*, 19,373, 1992.

Senior, C., D. Fontaine, G. Caudal, D. Alcaydé,, and J. Fontanari, Convection electric fields and electrostatic potential over $61° < \lambda < 72°$ invariant latitude observed with the European incoherent scatter facility, 2, Statistical results, *Ann. Geophys.*, *8*, 257, 1990.

Sibeck, D., R.E. Lopez,, and E.C. Roelof, Solar wind control of the magnetopause shape, location, and motion, *J. Geophys. Res.*, *96*, 5489, 1991.

Siscoe, G.L., and T.S. Huang, Polar cap inflation and deflation, *J. Geophys. Res.*, *90*, 543, 1985.

Spreiter, J.R., A.L. Summers,, and A.Y. Alksne, Hydrodynamic flow around the magnetosphere, *Planet. Space Sci.*, *14*, 223, 1966.

Stauning, P., C.R. Clauer, T.J. Rosenberg, E. Friis-Christensen,, and R. Sitar, Observations of solar-wind-driven progression of interplanetary magnetic field B_y-related dayside ionospheric disturbances, *J. Geophys. Res.*, *100*, 7567, 1995.

Taylor, J.R., T.K. Yeoman, M. Lester, B.A. Emery,, and D.J. Knipp, Variations in the polar cap area during intervals of substorm activity on 20-21 March 1991 deduced from AMIE convection patterns, *Ann. Geophysicae*, *14*, 879, 1996.

Todd, H., S.W.H. Cowley, M. Lockwood, D.M. Willis,, and H. Lühr, Response time of the high-latitude dayside ionospheric convection to sudden changes in the north-south component of the IMF, *Planet. Space Sci.*, *36*, 1415, 1988.

Weimer, D.R., L.A. Reinleitner, J.R. Kan, L. Zhu,, and S.-I. Akasofu, Saturation of the auroral electrojet current and the polar cap potential, *J. Geophys. Res.*, *95*, 18,981, 1990.

Weimer, D.R., Models of high-latitude electric potentials derived with a least error fit of spherical harmonic coefficients, *J. Geophys. Res.*, *100*, 19,595, 1995.

C. R. Clauer and V. O. Papitashvili, Space Physics Research Laboratory, University of Michigan, Ann Arbor, MI 48109. (e-mail: clauer@zasu.sprl.umich.edu; papita@zasu.sprl.umich.edu)

G. Lu, High Altitude Observatory, National Center for Atmospheric Research, Boulder, CO 80703. (e-mail: ganglu@hao.ucar.edu)

A. J. Ridley, Southwest Research Institute, 6220 Culebra Road, San Antonio, TX 78238-5166. (e-mail: ridley@worf.space.swri.edu)

(Received August 5, 1997; revised October 24,1997; accepted November 13, 1997.)